International Journal of Scientific & Engineering Research, Volume 8, Issue 2, February-2017
ISSN 2229-5518

Ultra-Wideband Channel Statistical Characterization in Different Laboratories

Hasna Chaibi*
has.chaibi@gmail.com

March 6, 2017

Abstract

Previous UWB channel characterizations have been reported for various frequency bands predominantly for several environments. We present residential characterizations different bandwidths 6 GHz 11 GHz, covering the spectrum under consideration by the FCC for UWB overlay systems. In this report we present the different statistics distribution can be used to describe the channel magnitude and phases behavior in frequency domain. We fond that the Weibull, Lognormal and nonparametric fit well with the pdf of the channel magnitude and nonparametric distribution fits well with the channel phases. Also, we evaluate the channel degrees of freedom evolution and channel entropy with channel bandwidth based on the channel measurements. First, we present the channel magnitude and phases in frequency domain under LOS and NLOS. Secondly, we present the channel degrees of freedom (DoF) evolution versus bandwidth under LOS and NLOS. Finally, a brief study of a well know channel parameter namely entropy is drawn.

Key words: UWB channel propagation, Indoor, Degrees of Freedom.

1 Introduction

Ultra–wideband (UWB) systems are now up-and-coming across a variety of commercial and military applications, including communications, radar, geolocation, and medical. First generation commercial wireless UWB products are anticipated to be widely deployed soon. This has been fueled by a demand for high frequency utilization and a large number of users requiring simultaneous multidimensional high data rate access for applications of wireless internet and e-commerce.
UWB systems are often defined as systems that have a relative bandwidth that is larger than 25% and/or an absolute bandwidth of more than 500 MHz (FCC) [1]. The UWB using large absolute bandwidth, are robust to frequency-selective fading, which has significant implications on both, design and implementation, Among the important characteristics of the UWB technology are low power devices, accurate localization, a high multipath immunity, low complexity hardware structures and carrier-less architectures [2]. The goal of this report is to: First, present some statistical distributions that can be presents a best fit for measured UWB channel conducted at different laboratories. Secondly, we analyze the impact of these extremely large systems bandwidth on the covariance matrix channel based on measurements conducted at Eurecom, Intel and IMST.

The rest of the paper is organized as follows. Section 2 presents the steps taken to go from measured data and component characterization to the estimate of channel parameters and describes the channel behavior frequency domain. In Section 3 we outline the covariance matrix estimation and we present first results about sub-space analysis, evolution of DoF and the channel entropy. Section 4 ends the paper.

*Hasna Chaibi is a Phd. from ENSIAS, Mohammed V University, Rabat, Morocco.

2 UWB channel measured data considerations and statistical distribution

In this section we describe the steps taken to go from measured data and component characterization to the estimate of channel parameters. In the case of the frequency domain collection the compensation was applied directly to network analyzer data. The inverse Fourier transform was then used to generate the estimate of the channel impulse response. Measurements from the network analyzer (NWA) were used to estimate the channel frequency response, and thus the channel impulse response by inverse Fourier transform. Letting $P(jw)$ represent the Fourier transform the non-ideal components (amplifiers, filters, antennas, etc., but no pulser) between the NWA outputs and inputs, we see that the spectrum $Y(jw)$ measured by the network analyzer is equal to

$$P(jw)H(jw) + N(jw) = Y(jw) \tag{1}$$

where $H(jw)$ is the channel impulse response and $N(jw)$ is an additive white Gaussian noise (AWGN) that includes all noise sources including errors in component compensation.

The minimum mean square error (MMSE) estimate of the frequency response is thus

$$\hat{H}(jw_i) = \frac{Y(jw_i)}{P(jw_i)} \tag{2}$$

where w_i[1] are the tones used by the network analyzer to probe the channel. We call the ratio in equation (2) the measured signal after compensation for non-ideal components. Here $N(jw)$ represents both the measurement noise and the error in our characterization of the non-ideal components; and we model this noise as being AWGN. Note that we can also analyze data collected by the digitizing oscilloscope using this frequency domain approach, where $P(jw)$ represents the pulser as well as the other components. Note that any frequency domain windowing will increase the mean square error of the channel estimates. However, for the purposes of counting the number of multiple paths, and to avoid leaking of energy of one path to the next, various types of frequency domain windows have been used in channel measurements [5, 6]. In this study we evaluate the channel parameters without windowing (a rectangular window is applied on all measurements).

2.1 Statistical distributions background

To characterize the probability density function of the power variations in frequency domain ($H(f)$) we plot the histogram's measurement data. The power variations are fitted with an analytical probability density function (pdf) approximation, namely a Weibull pdf and Lognormal pdf. The general formula for the Weibull pdf is given by:

$$f(z) = \frac{\gamma}{\alpha}\left(\frac{z-\mu}{\alpha}\right)^{(\gamma-1)} \exp\left\{-\left(\frac{z-\mu}{\alpha}\right)^{\gamma}\right\} \tag{3}$$

where α, γ, $\mu \in R$, $\alpha, \gamma > 0$ and $z \geq \mu$, α is the scale parameter, γ is the shape parameter, and μ is the location parameter.

The general formula for the Lognormal pdf is given by:

A variable X is lognormally distributed if $Y = \log(X)$ is normally distributed with log denoting the natural logarithm. The general formula for the probability density function of the lognormal distribution is

$$f(x) = \frac{1}{\sigma\sqrt{2\pi}(x-\theta)} \exp(-\frac{[\ln\frac{x-\theta}{m}]^2}{2\sigma^2} \quad x \geq \theta; \quad \sigma, \quad m > 0. \tag{4}$$

where σ is the shape parameter, θ is the location parameter and m is the scale parameter. The case where $\theta = 0$ and $m = 1$ is called the **standard lognormal distribution**.

[1] $jw_k = f_k$

2.2 UWB channel measurements: setup and environments

The used UWB channel measurement companies in this report are.

1. Eurecom UWB channel measurements [16].
2. Intel UWB channel measurements.
3. IMST UWB channel measurements.

In follows a short description of all used channel measurements.

2.2.1 Eurecom measurements (Frequency domain 2003–2004)[16]

Measurements are performed at spatially different locations under both Line-of Sight (LOS) and Non Line of Sight (NLOS). The experiment area is set by fixing the transmitting antenna on a mast at 1 m above the ground on horizontal linear grid (20 cm) close to VNA and moving the receiver antenna to different locations on horizontal linear grid (50 cm) in 1 cm steps. The height of the receiver antenna was also 1 m above the ground. This configuration targets peer-to- peer applications. Among all positions, we consider both LOS and NLOS configurations. Measurements are carried out in Eurecom Mobile Communication Laboratory, which has a 2 typical laboratory environment (radio frequency equipment, computers, tables, chairs, metallic cupboard, glass windows,...) with plenty of reflective and diffractive objects, as shown in Fig. 2 and Fig. 3, rich in reflective and diffractive objects [16]. For the NLOS case, a metallic plate is positioned between the transmitter and the receiver. We have complete database of 4000 channel frequency responses corresponding to different scenarios with a transmitter-to-receiver distance varying distance varying from 1 meter to 14 meters. The attenuation and the phase of the channel response has been measured from 3 to 9 GHz with a 1 MHz frequency spacing.

2.2.2 Intel measurements (Frequency domain 2001)

David Cheung et al. are performed over 2100 measurements over a period of three months in the summer of 2001. Roughly half of these measurements were made in a residential environment a townhouse in Oregon. The rest were taken in an office environment and in an anechoic chamber. They are consider this townhouse to be a reasonable representation of the residential environment. The townhouse has two floors and measures roughly 13.5 m in length and 5 m in width. An Intel study on 802.11b path loss had been made previously in this same townhouse [8]. An Agilent 8720ES S-Parameter Network Analyzer (NWA) is used for channel transfer function (frequency domain) measurements and a Tektronix TDS8000 Digital Sampling Oscilloscope for channel impulse response (time domain) measurements and characterized propagation effects over a frequency range of $2-8$ GHz. In our analysis juste the measurements in frequency domain are exploited.

2.2.3 IMST measurements (Frequency domain 2002)

For IMST measurements the measured data obtained during an indoor UWB measurement campaign that has been performed at IMST premises in 2001 within the whyless.com project. All the radio channel measurements have been performed at the IMST premises within an office with the dimensions 5 m $\times$ 5 m $\times$ $2-6$ m. The office has a single door, one wall with windows, and contains a metal cabinet. Both the transmitter and receiver deploy a biconical horn antenna with approx. 1 dBi gain, which is positioned at a height of 1.5 m. The attenuation and the phase of the channel response has been measured from 1 to 11 GHz with a 6.25 MHz frequency spacing. The antennas are considered part of the radio channel. To measure the small-scale fading, the transmitter position has been moved over a 31×151 grid with 1 cm spacing, while the receiver position remained constant. The receiver is directly visible all over the grid. Successively, both the receiver position and the transmitter grid have been moved within the office such that the metal cabinet obstructs the LOS path all over the grid. The measurement has been repeated as described before and will be denoted to as the NLOS measurement. The measurement set-up and results are described more in detail in [7].

2.3 Evaluation

As we can see from different Figures on 1 and 2 the lognormal with diffrent values of σ fits very well with the all measurements from IMST (LOS and NLOS for different settings), Eurecom outdoor (LOS 6 meters between antennas) and intel (for different settings and locations) expected those token with antennas distance separation less than 2 meters are fitted with an Weibull distribution. On the other hand the Weibull fits very well with measurements from Eurecom for all settings (LOS and NLOS in indoor laboratory or corridor). Figure 3 shows the channel phases distribution for different channel situations. The phases for all channels can be presented by a nonparametric distribution.

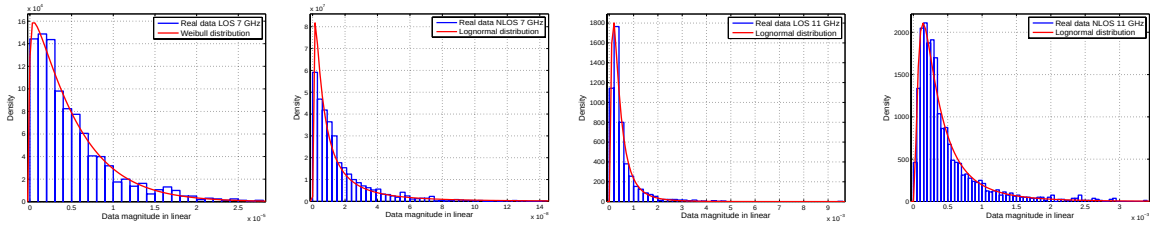

(a) Intel LOS (b) Intel NLOS $\sigma = 2$ (c) IMST LOS $\sigma = 1.78$ (d) IMST NLOS $\sigma = 1$

Figure 1: Magnitude distribution for LOS and NLOS Intel and IMST measurements.

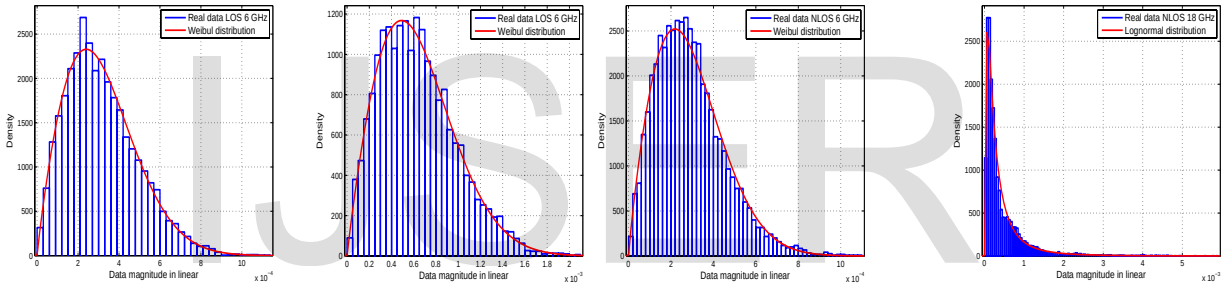

(a) Eurecom LOS corridor (b) Eurecom LOS Eurecom LOS (c) Eurecom LOS outdoor $\sigma = 1.8$

Figure 2: Magnitude distribution for LOS and NLOS Eurecom.

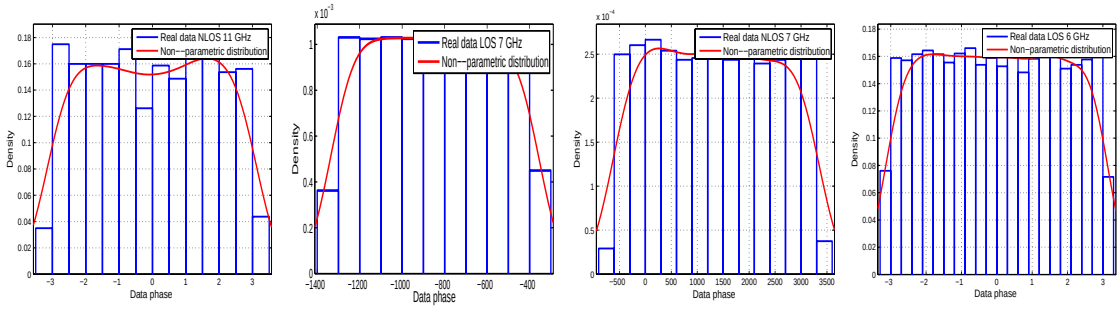

(a) IMST NLOS (b) Intel LOS (c) Intel NLOS (d) Eurecom LOS

Figure 3: Phases distribution for LOS and NLOS IMST, Intel, Eurecom outdoor measurements.

3 UWB channel sub space eigen–decomposition Preliminary results

In The Section

3.1 Mathematical formulation

The covariance matrix is Hermitian and positive definite. For this reason, a unitary matrix $\mathbf{U_h}$ exists such that the Karhunen-Loève (KL) expansion gives [16] :

$$\mathbf{K}_{\mathbf{h}}^{N} = \mathbf{U_h}\Lambda_{\mathbf{h}}\mathbf{U}_{\mathbf{h}}^{H} = \sum_{i=1}^{N} \lambda_i(\mathbf{h})\psi_i(\mathbf{h})\psi_i^H(\mathbf{h});\ \mathbf{U}_{\mathbf{h}}^{H}\mathbf{U_h} = \mathbf{I}_N, \tag{5}$$

where $\lambda_1(\mathbf{h}) \geq \lambda_2(\mathbf{h}) \geq ... \geq \lambda_N(\mathbf{h})$, $\psi_i(\mathbf{h})$ is the i^{th} column of $\mathbf{U_h}$ and $\mathbf{I}_N$ is the $N \times N$ identity matrix with N number of samples. $\lambda_i(\mathbf{h})$ and $\psi_i(\mathbf{h})$ are the i^{th} eigenvalues and eigenvectors of $\mathbf{K}_{\mathbf{h}}^{N}$, respectively. Decomposing $\mathbf{U_h}$ into principal and noise components yields

$$\begin{gathered}\mathbf{U}_{s,\mathbf{h}} = [\psi_1(\mathbf{h}), \psi_2(\mathbf{h}), ..., \psi_p(\mathbf{h})];\\ \lambda_1(\mathbf{h}) \geq \lambda_2(\mathbf{h}) \geq ... \geq \lambda_L(\mathbf{h});\\ \mathbf{U}_{n,\mathbf{h}} = [\psi_{L+1}(\mathbf{h}), \psi_{L+2}(\mathbf{h}), ..., \psi_N(\mathbf{h})];\\ \lambda_{L+1}(\mathbf{h}) \geq \lambda_{L+2}(\mathbf{h}) \geq ... \geq \lambda_N(\mathbf{h}).\end{gathered}$$

where $\mathbf{U}_{s,\mathbf{h}} \perp \mathbf{U}_{n,\mathbf{h}}$. $\mathbf{U}_{s,\mathbf{h}}$ defines the subspace containing both signal and noise components, whereas $\mathbf{U}_{n,\mathbf{h}}$ defines the noise-only subspace [16].

3.2 Number of DoF evalution based on the % of captured energy

The above mathematical formulation is applied to evaluate the UWB channel eigen-values distribution with channel bandwidth. Our analysis is used to compute the significant eigenvalues, we apply this on UWB channel measurements conducted at Eurecom. The bandwidth of interest here is from 3 GHz to 5 GHz. Figure 4 shows that the number of DoF increases with channel bandwidth but not linearly. For example we fix the percentage of received energy on 98% the number of DoF is depicted on Figure 6 [16], This figure is considered for comparaison. The figure 6 shows that we can approximate the channel DoF evolution with frequency bandwidth by

$$f(F) = A\log(F) \tag{6}$$

where A is a constant and F is the frequency bandwidth. For 95% of received energy we can represent the DoF evolution by $4.7\log(F)$. Because of the band-limiting nature of the Ultra Wide bandwidth channels, the channel will be characterized by a finite number D of significant eigenvalues, which for rich environments will be close to $N = 1+2WT_d$, in the sense that a certain proportion of the total channel energy will be contained in these D components. Based on measurement campaigns described above and Figures on 4, 5 and 6 we see that the number of significant eigenvalues can be large but significantly less than the approximate dimension of the signal-space $1 + 2WT_d$ Chapter 8 in [18]. This is due to insufficient scattering in short range indoor environments. For notational convenience, we will assume that the eigenvalues are ordered by decreasing amplitude.

3.3 Empirical Entropy evaluation

The entropy is a measure of disorder of a system. Our system is the UWB channel and the disorder concerns the independent paths in this channel. As discuss above $\hat{R}$ is the estimated covariance matrix and the $\hat{\lambda}_k$ is the k^{th} eigenvalues of $\hat{R}$ and $\sum_k \hat{\lambda}_k = 1$. In [Tsuda *et al.*, 2004] the Von Neumann entropy is given by $E(K) = -\mathrm{tr}[\hat{R}\log\hat{R}]$, in this work and the Von Neumann Entropy presents the Shannon entropy of eigenvalues.
Let $\hat{S}$ the empirical entropy

$$\hat{S} = -\mathrm{tr}[\hat{R}\log\hat{R}] = -\sum_{k=1}^{L} \hat{\lambda}_k \log\hat{\lambda}_k \tag{7}$$

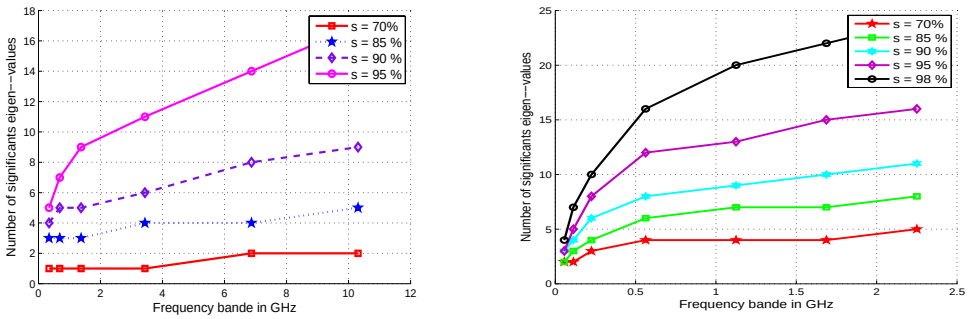

(a) IMST NLOS (b) D. Eurecom Outdoor LOS

Figure 4: DoF evolution versus channel bandwidth for NLOS cases for different captured energy thresholds IMST and Eurecom outdoor measurements.

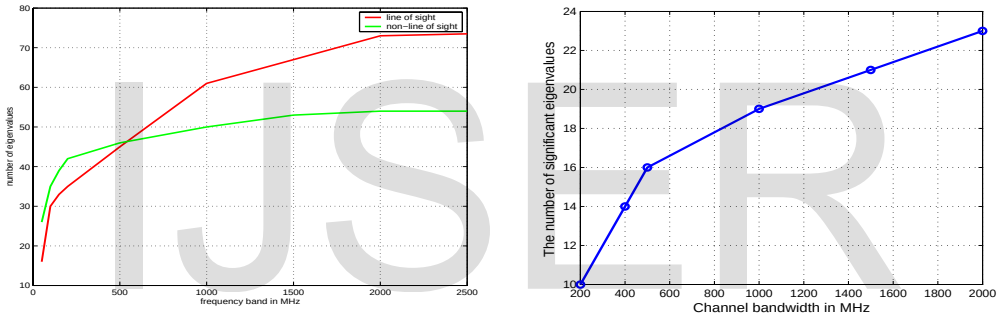

(a) Eurecom LOS and NLOS [16] (b) Eurecom Outdoor LOS

Figure 5: DoF evolution versus channel bandwidth.

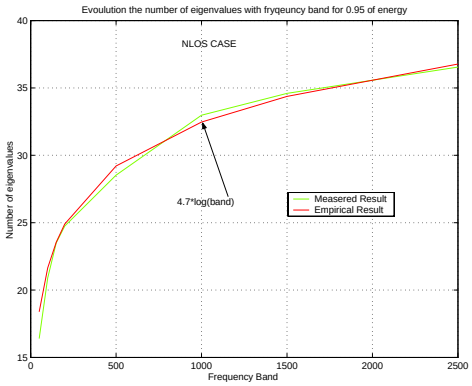

Figure 6: DoF evolution versus channel bandwidth for 95% of captured energy.

we call $\hat{S}$ empirical entropy because it is calculated based on estimated eigenvalues from a given set of channel measurements.

To confirm the results presented previously in the channel DoF saturation versus the channel bandwidth. We evaluate the channel entropy $\hat{S}$ for both LOS and NLOS settings.

In Figure 7, the channel entropy $\hat{S}$ is plotted for both LOS and NLOS scenarios with respect to the channel frequency band width. From this figure, we can see that the $\hat{S}$ under NLOS case is greater than the $\hat{S}$ found under LOS one. This result confirms that the uncertainty increases with NLOS conditions which is due to the generation of supplementary multipaths under this environment. Figure 7 shows also that, the channel entropy $\hat{S}$ increases with the frequency bandwidth but not linearly which confirms the saturation and the sub-linear behavior found previously of the DoF.

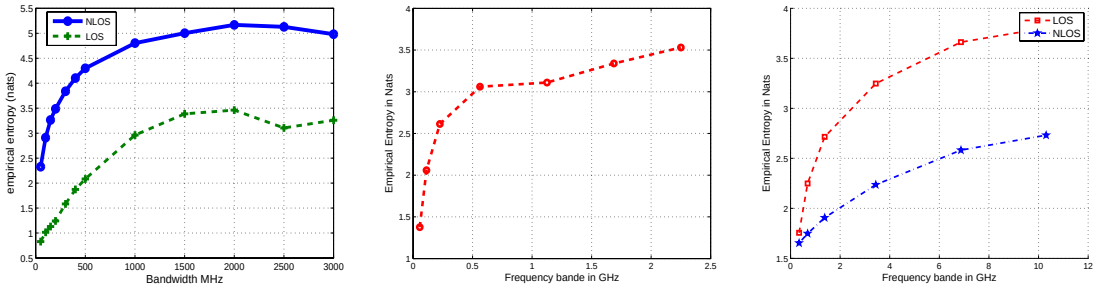

(a) Eurecom LOS NLOS (b) Eurecom Outdoor NLOS (c)IMST LOS and NLOS

Figure 7: Channel empirical entropy in NLOS and LOS cases for different channel measurements laboratories.

3.4 Number of DoF estimations on the basis AIC, MDL and BIC

AIC and MDL are model-order determination algorithms that can also be used for determining how many signals are present in vector valued data. Suppose the $M \times 1$ complex vector $h(t)$ can be modeled as

$$h(t) = As(t) + n(t) \tag{8}$$

A is a rank(P) $M \times P$ complex matrix whose columns are determined by the unknown parameters associated with each signal. $s(t)$ is a $P \times 1$ complex vector whose p^{th} element is the waveform of the p^{th} signal, and n(t) is a complex, stationary, and ergodic Gaussian process with zero mean and covariance matrix $E\{n(t)n'(t)\} = \sigma_n^2 I_n$. The problem is to determine P from N observations of $h(t)$; i.e., $h(t_1), ..., h(t_N)$. Let

$$\mathbf{R} = E\{h(t)h'(t)\}. \tag{9}$$

be the covariance matrix of the data $h(t)$, and

$$\hat{\mathbf{R}} = \frac{1}{N}\sum_{i=1}^{N} h(t_i)h'(t_i). \tag{10}$$

$\hat{\mathbf{R}}$ be an estimate of $\mathbf{R}$.

The covariance matrix is Hermitian and positive definite. For this reason, an unitary matrix $\mathbf{U_h}$ exists such that the Karhunen-Loève (KL) expansion gives

$$\mathbf{R} = \mathbf{U_h}\Lambda_\mathbf{h}\mathbf{U}_\mathbf{h}^H = \sum_{i=1}^{N} \lambda_i(\mathbf{h})\psi_i(\mathbf{h})\psi_i^H(\mathbf{h});\ \mathbf{U}_\mathbf{h}^H\mathbf{U_h} = \mathbf{I}_N, \tag{11}$$

where $\lambda_1(\mathbf{h}) \geq \lambda_2(\mathbf{h}) \geq ... \geq \lambda_N(\mathbf{h})$, $\psi_i(\mathbf{h})$ is the i^{th} column of $\mathbf{U_h}$ and $\mathbf{I}_N$ is the $N \times N$ identity matrix with N number of samples. $\lambda_i(\mathbf{h})$ and $\psi_i(\mathbf{h})$ are the i^{th} eigenvalues and eigenvectors of $\mathbf{R}$, respectively.

Furthermore, if P uncorrelated signals are present, the $M-P$ smallest eigenvalues of $\mathbf{R}$ are all equal to the noise power σ_n^2, and the vector of parameters $\Theta^{(P)}$ specifying $\mathbf{R}$ can be written as

$$\Theta^{(P)} = [\lambda_1, \lambda_2, ..., \lambda_{P-1}, \lambda_P, \sigma_n^2, \psi_1^T, \psi_2^T, ..., \psi_P^T] \tag{12}$$

The number of signals are determined from the estimated covariance matrix $\hat{\mathbf{R}}$. In the [19] the AIC criteria was adapted for detection of the number of signals. This procedure is recalled here in simplified form.
If $\hat{\lambda_1}, \hat{\lambda_2}, ..., \hat{\lambda_M}$ are the eigenvalues of $\hat{\mathbf{R}}$ in the decreasing order then

$$AIC(k) = -2\log\left(\frac{\prod_{i=k+1}^{p}\lambda_i(\mathbf{h})^{\frac{1}{(p-k)}}}{\frac{1}{p-k}\sum_{i=k+1}^{p}\lambda_i(\mathbf{h})}\right)^{N(p-k)} + 2k(2p-k) \tag{13}$$

and

$$MDL(k) = -\log\left(\frac{\prod_{i=k+1}^{p}\lambda_i(\mathbf{h})^{\frac{1}{(p-k)}}}{\frac{1}{p-k}\sum_{i=k+1}^{p}\lambda_i(\mathbf{h})}\right)^{N(p-k)} + \log(N)\frac{k(2p-k+1)}{4} \tag{14}$$

The number of degrees of freedom, possibly the number of significant eigenvalues, is determined as the value of $k \in \{0, 1, ..., p-1\}$ which minimizes the value of (13) or (14). In this study the number of DoF represents the number of unitary dimension independent channels that constitute an UWB channel.

We have also applied HQ criterion to evaluate the number of significants eigen values in the channel:

$$HQ(k) = -L(\hat{\theta}) + \frac{1}{2}k(2p-k)\log(\log(N)) \tag{15}$$

where $L(\hat{\theta})$ is the log-likelihood function f which is given by:

$$L(\hat{\theta}) = \log\left(\frac{\prod_{i=k+1}^{p}\lambda_i^{\frac{1}{p-k}}}{\frac{1}{p-k}\sum_{i=k+1}^{p}\lambda_i}\right)^{N(p-k)} \tag{16}$$

The number of significant eigenvalues is the value of k for which the HQ criteria is minimized. Figure 8

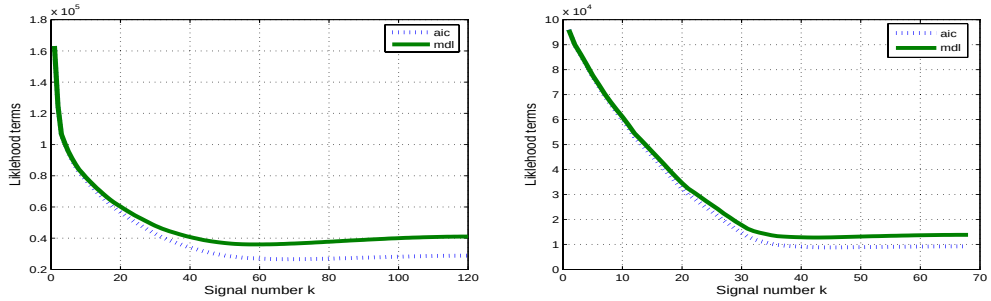

(a) AIC and MDL Eurecom LOS (b) AIC and MDL Eurecom LOS

Figure 8: AIC and MDL for eurecom measurements.

considers LOS and NLOS measurements settings, we plot the AIC and MDL functions for channel bandwidth typically 6 GHz. The minimum of AIC or MDL curves give the number of significant eigenvalues. As a matter of fact, we see that the number of DoF increases with bandwidth but not linearly, the "Table 1 " summarized a some value of k that minimizes the AIC and MDL criterion. Thus, for 200 MHz bandwidth, we capture 98% of the energy with 29 significant eigenvalues see (a) on Figure 5 whereas for 6 GHz channel bandwidths the number of eigenvalues is 50.

As the number of DoF not increase linearly with the band then it is not interesting to exploit entirely the band authorized by the FCC to transmit one information. According to the analysis presented in top a

Table 1: The values of k minimize AIC and MDL

	Settings			
	LOS		NLOS	
ΔW	200 MHz	6 GHz	200 MHz	6 GHZ
k_{AIC}	23	68	25	46
k_{MDL}	21	60	23	42
k_{HQ}	24	69	25	48

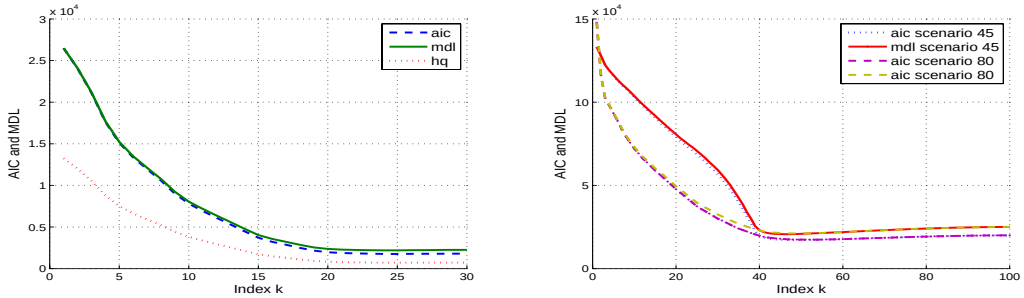

(a) AIC, MDL and HQ Eurecom outdoor LOS (b) AIC and MDL IMST LOS

Figure 9: AIC, MDL and HQ for Eurecom outdoor LOS and IMST measurements.

saturation of DoF take place from 1 GHz. For better exploiting the authorized band it should be divided into sub–bands. Finnaly, we have shown providently in [16] that the relationship between the number of significant eigenvalues and the τ_{rms} delay spread is given by the following equation:

$$\tau_{rms} = \frac{k}{W}, \tag{17}$$

where W is the frequency band. To evaluate the τ_{rms} delay spread for our measurements we use (17), and by taking $k = 23$ this corresponds $W = 200$ and 46 ns (Eurecom measurements LOS).

3.5 Recommendation

Based on the analysis above, we noticed that beyond a value of the bandwidth of the channel, most of the time about 500 MHz, the number of values propors tends towards saturation. This result is very important for proper sizing of the band. For example instead of using the entire 7.5 GHz band to send a single information, we can sub-divide the band into 15 sub-band width 500 MHz. This allows us to send 15 times more information.

4 Conclusion

In this report, we have present an set of results concern UWB channel measurements for different laboratories. The measurement are performed in the frequency domain. First we have present some results about the magnitude and channel phases distribution. We found that the data fit well with Weibull and lognormal distribution (magnitude) and a non parametric distribution is reported to fit all data phases. Secondly, we have interested to DoF channel evaluation with the channel bandwidth. We have shown that the AIC, MDL and HQ are three techniques to estimate the number of DoF of an UWB channel in an in-door environment. This DoF evaluation using different techniques, highlights that the number of DoF for a given UWB channel saturates beyond a certain frequency bandwidth and does not increase linearly. Also an estimation of the entropy parameter is provided to justify the DoF behavior with the channel bandwidth.

5 Acknowledgements

I would like to first say a very big thank you to Professor **Rachid Saadane** for all the support and encouragement he gave me. Without her guidance and constant feedback this report would not have been achievable. Many thanks also to Phd. **Zakaria Mohammadi** who convinced me during our many discussions about UWB channel measurements. Many thanks to all the laboratories to which the measurements were made, mainly Intel, IMST and Eurecom.

References

[1] First report and order, revision of part 15 of the commission's rules regarding ultra-wideband transmission systems, ET Docket 98–153.

[2] R. J.-M. Cramer, R. A. Scholtz, and M. Z. Win, "Evaluation of an ultra-wide-band propagation channel," *IEEE Transactions on Antennas and Propagation*, vol. 50, no. 5, pp. 561-570, May 2002.

[3] M. J. E. Golay."Notes on digital coding," in *Proc. IRE,* **37**, 657, 1949.

[4] I. E. Telatar and D. N. C. Tse."Capacity and Mutual Information of Wideband Multipath Fading channels," in *Trans. on Information Theory,* **2**(2), 1384–1400, 2000.

[5] Hashemi, H., "The indoor radio propagation channel," *Proceedings of the IEEE,* vol. 81, no. 7, pp. 943-968 July 1993.

[6] Hashemi, H., "Impulse response modeling of indoor radio propagation channels," *IEEE Journal on Selected Areas in Communications,* vol. 11, no. 7, pp. 967-978, Sept. 1993.

[7] J. Kunisch and J. Pamp, "Measurement results and modeling aspects for the UWB radio channel," in *IEEE Conference on Ultra Wideband Systems and Technologies Digest of Technical Papers*, Baltimore, MD, USA, May 2002, pp. 19-23.

[8] Peek, Greg and Ryan Etzel, 802.11b coexistence results (5 PDF files discussing interference with Bluetooth, cordless phone, and 802.11b), Intel, May through July 2001. http://people1.patch.intel.com/gpeek/coexistence/home.htm,,

[9] A. Alvarez, G. Valera, M. Lobeira, J. L Garcia, "New channel impulse response model for UWB indoor system simulations," *IEEE Vehicular Technology Conference* - Spring, Jeju, Korea, pp. 1-5, May 2003.

[10] S. Ghassemzadeh, L. Greenstein, T. Sveinsson, A. Kavcic, V. Tarokh, "UWB indoor path loss model for residential and commercial environments," in Proc. IEEE Veh. Technol. Conf (VTC 2003- Fall), Orlando, FL, USA, Sep 2003, pp. 629-633.

[11] L. Rusch, C. Prettie, D. Cheung, Q. Li, M. Ho, "Characterization of UWB propagation from 2 to 8 GHz in a residential environment," 2003,[Online]. Available: www.intel.com.

[12] C.-C. Chong, Y. Kim, S.-S. Lee, "Statistical characterization of the UWB propagation channel in various types of high-rise apartments," Wireless Communications and Networking Conference, March 2005, pp:944 - 949.

[13] A.F. Molisch, B. Kannan, C. C. Chong, S. Emami, A. Karedal, J. Kunisch, H. Schantz, U. Schuster and K. Siwiak, "IEEE 802.15.4a Channel Model- Final Report," IEEE 802.15-04-0662-00-004a, San Antonio, TX, USA, Nov.2004.

[14] A. Molisch, "Time Variance for UWB Wireless Channels," submitted to the IEE P802.15 Working Group for Wireless Personal Area Networks (WPANs) on 11 Nov, 2002.

[15] D. Cassioli, M. Z. Win, and A. F. Molish. " The ultra-wide bandwidth indoor channel-from statistical model to simulation," *IEEE Journal on Selected Areas Communications*, **2**(2), 1247–1257.

[16] R. Saadane, A. Menouni Hayar, R. Knopp, D. Aboutajdine, "On the estimation of the degrees of freedom of in-door UWB channel," *VTC Spring 2005, 61st Vehicular Technology Conference,* Stockholm, Sweden, 29th May - 1st June, 2005.

[17] D. Tse, and P. Viswanath, Fundamentals of Wireless Communication. Cambridge University Press, May 2005.

[18] R. G. Gallager, Information Theory and Reliable Communication. Wiley and Sons, New York, 1968.

[19] M. Wax and T. Kailath, "Detection of Signals by Information Theoretic Criteria", *IEEE Trans. on Acoustics,Speech, and Signal Processing,* vol. ASSP-33, No. 2, April 1985, pp. 387-392.